

# Cyclic electron flow under saturating excitation of dark-adapted Arabidopsis leaves

Pierre Joliot\*, Daniel Béal, Anne Joliot

*Institut de Biologie Physico-Chimique, CNRS UPR 1261, 13, rue Pierre-et-Marie Curie, 75005 Paris, France*

Received 22 October 2003; received in revised form 12 March 2004; accepted 25 March 2004

Available online 26 April 2004

## Abstract

The rate of cyclic electron flow measured in dark-adapted leaves under aerobic conditions submitted to a saturating illumination has been performed by the analysis of the transmembrane potential changes induced by a light to dark transfer. Using a new highly sensitive spectrophotometric technique, a rate of the cyclic flow of  $\sim 130 \text{ s}^{-1}$  has been measured in the presence or absence of 3-(3,4-dichlorophenyl)-1,1-dimethylurea (DCMU). This value is  $\sim 1.5$  times larger than that previously reported [Proc. Natl. Acad. Sci. U. S. A. 99 (2001) 10209]. We have characterized in the presence or absence of DCMU charge recombination process ( $t_{1/2} \sim 60 \mu\text{s}$ ) that involves  $\text{P}_{700}^+$  and very likely the reduced form of the iron sulfur acceptor  $\text{F}_X$ . This led to conclude that, under saturating illumination, the PSI centers involved in the cyclic pathway have most of the iron sulfur acceptors  $\text{F}_A$  and  $\text{F}_B$  reduced. In the proposed mechanism, electrons are transferred from a ferredoxin bound to a site localized on the stromal side of the cytochrome  $b_6/f$  complex to the  $\text{Q}_i$  site. Two possible models of the organization of the membrane complexes are discussed, in which the cyclic and linear electron transfer chains are isolated one from the other.

© 2004 Elsevier B.V. All rights reserved.

**Keywords:** Cyclic electron flow; Photosystem I; Cytochrome  $b_6/f$ ; Arabidopsis

## 1. Introduction

The occurrence of cyclic phosphorylation in isolated thylakoids membranes was first demonstrated by Arnon et al. [1] when a light-induced efficient ATP synthesis was observed in the absence of oxygen and in the presence of catalytic amounts of vitamin K. As this process is not associated with oxygen formation or consumption and as its efficiency is increased by the addition of 3-(3,4-dichlorophenyl)-1,1-dimethylurea (DCMU), it involves cyclic electron transfer around Photosystem (PS) I. In addition to vitamin K, several nonphysiological agents as phenazine

methosulfate (PMS) have been shown to catalyze an efficient cyclic photophosphorylation [2]. It was proposed that all these cofactors were involved in the transfer of electron from the acceptor side of PSI to an electron transfer chain including cytochrome (cyt)  $b$  and cyt  $f$ . Later, it was demonstrated that the cyclic phosphorylation process can also be catalyzed by the addition of ferredoxin (Fd) [3], previously identified as the primary soluble physiological electron acceptor involved in linear electron flow [4]. In the presence of oxygen, efficient linear electron flow is observed whereas cyclic electron flow was better observed under anaerobic condition, i.e. in conditions where Fd is not reoxidized by oxygen.

Demonstrating that a cyclic process leads to ATP synthesis in leaves or intact chloroplasts is a more difficult task, mainly for technical reasons; reviewed in Refs. [5,6]. Moreover, a cyclic flow is often difficult to distinguish from a pseudo-cyclic process able to generate ATP, in which electrons are transferred from water to oxygen via the acceptor side of PSI [7,8]. It has been reported [9,10] that a decrease of  $\text{CO}_2$  concentration stimulates a cyclic electron flow, or conversely, that no significant cyclic flow occurs during the induction period or in the absence of  $\text{CO}_2$  [11].

*Abbreviations:*  $\text{A}_1$ , Photosystem I phylloquinone acceptor; cyt  $b/f$ , cytochrome  $b_6/f$ ; cyt, cytochrome; DCMU, 3-(3,4-dichlorophenyl)-1,1-dimethylurea; Fd, ferredoxin; FNR, ferredoxin-NADP reductase;  $\text{F}_X$ ,  $\text{F}_A$ ,  $\text{F}_B$ , iron sulfur Photosystem I secondary acceptors; LED, light-emitting diode; NDH, NADP dehydrogenase; NPQ, non-photochemical quenching;  $\text{P}_{700}$ , PSI primary donor; PC, plastocyanin; PMS, phenazine methosulfate; PQ, plastoquinone;  $\text{PQH}_2$ , plastoquinol; PS, Photosystem; RC, reaction center

\* Corresponding author. Tel.: +33-1-58-41-50-44; fax: +31-14-46-83-31.

*E-mail address:* [pjoliot@ibpc.fr](mailto:pjoliot@ibpc.fr) (P. Joliot).

From the analysis of the temperature dependence of PSI and PSII electron transfer rates in the presence of CO<sub>2</sub>, it was concluded that the contribution of cyclic electron flow rises with falling temperature [12]. From non-photochemical quenching (NPQ) measurements, a significant cyclic electron flow was observed under far red light excitation and at low CO<sub>2</sub> and O<sub>2</sub> concentrations [13]. Efficient energy storage ascribed to a cyclic electron flow has been reported from photoacoustic measurements under far-red excitation in anaerobic conditions. The half time of P<sub>700</sub><sup>+</sup> reduction in the dark was ~ 400 ms, which corresponds to a rate of cyclic flow of ~ 2 s<sup>-1</sup> [14].

Arguments that favor the occurrence of a cyclic process are provided by the structural organization of the thylakoids membrane in higher plants. It is well established that PSI and PSII centers are localized in different regions of the membrane, non-appressed and appressed, respectively [15], while *cyt f* is distributed in these two membrane regions [16]. The membrane proteins, which occupy more than half of the surface of the photosynthetic membrane, act as barriers that limit the diffusion of plastoquinone (PQ) [17–19], thus restricting it to domains including an average of two to four reaction centers (RC), a membrane surface much smaller than that of a grana membrane. On this basis, these authors exclude that quinone can be involved in long-range electron transfer processes between PSII and PSI. They conclude that the linear electron flow should involve exclusively the cytochrome *b<sub>6</sub>f* (*cyt b/f*) complexes localized within the appressed region of the membrane, i.e. at short distance of PSII. Long-range diffusion of electrons between the *cyt b/f* complex and PSI would be then mediated by plastocyanin (PC). *Cyt b/f* complexes localized in the non-appressed region of the membrane, and within a close distance to PSI, would be to participate to the cyclic electron flow. Thus, the segregation of PSI and PSII centers in different membrane regions provides a rationale for both a linear and a cyclic electron flow taking place in the photosynthetic process.

In a recent paper [20], the rate of the linear and cyclic flows during the first seconds of illumination of a dark-adapted spinach leaf in aerobic condition was estimated by measuring the rate of decay of the membrane potential at the time the light is switched off. Under strong illumination, the cyclic process operates at a rate of ~ 80 s<sup>-1</sup>. Moreover, a similar rate was found, at least transiently, in the presence of DCMU, i.e. in conditions where any contribution from the linear flow to the overall photochemical rate should be excluded. It was assumed that the cyclic electron transfer chain operates within a supercomplex including one PSI, one *cyt b/f* complex and a trapped Fd and PC, as previously proposed in Refs. [21–23]. Another fraction of PSI centers, not organized in supercomplex, would be involved in the linear pathway.

The occurrence of a cyclic flow can be rationalized by the need to increase the concentration of ATP that limits the rate of the Benson–Calvin cycle in dark-adapted leaves. It is thus likely that cyclic flow operates transiently and that for

increasing duration of illumination, the fraction of PSI participating in the cyclic flow decreases whereas that involved in the linear flow increases. The efficient cyclic flow that operates during the first seconds of illumination would be responsible for the rapid development of NPQ, which is known to be ΔpH-dependent [24]. Whereas most studies on the relative contribution of the cyclic flow to the photosynthetic process have been performed under steady-state conditions, we thus consider as important to focus on the transient state involved in the activation of the Benson–Calvin cycle.

In this paper, we describe a new spectrophotometric technique that allows more precise measurements of the time course of the membrane potential decay and of the rate of the cyclic flow. This technique provides a detailed analysis of the membrane potential decay and can be used in non steady-state conditions, at variance with the dark interval relaxation kinetics (DIRK) method developed earlier [25]. The experiments have been performed with *Arabidopsis* leaves under an illumination intensity that is close to be saturating for linear and cyclic process.

On the basis of these results, we discuss possible models for the mechanism of electron transfer involved in the cyclic electron flow and for the organization of membrane proteins within the thylakoids.

## 2. Materials and methods

The experiments were performed with leaves of *Arabidopsis thaliana*, ecotype Columbia. When stated, the leaf was infiltrated under low pressure with water or 0.15 M sorbitol in the presence or in the absence of 40 μM DCMU. The inhibition of PSII by DCMU was confirmed by fluorescence measurements. The gas composition of the cuvette can be controlled by pumping air over the surface of the leaf.

### 2.1. Spectrophotometric measurements

Measurements were performed with an apparatus similar to that described in [26,27] using xenon detecting flashes or with a new spectrophotometer using light-emitting diodes (LEDs) as detecting flashes and described in Fig. 1. LEDs are applied on a solid glass light pipe that realizes a first randomization of the light beam. The output of this glass light pipe is applied to a W-shaped fiber bundle, with randomly distributed fibers, used to illuminate the leaves by actinic and detecting light. The outputs of the light pipes (5 × 15 mm) are directly applied against the upper surface of each leaf. One of the leaves is used as the reference while the other is exposed to actinic illumination (measure).

The detecting flashes are provided by LEDs peaking at 485, 518 and 810 nm, respectively. At 485 and 518 nm, the bandwidth is ~ 35 nm. The intensity of the transmitted light is measured by two silicon photodiodes PIN Hama-

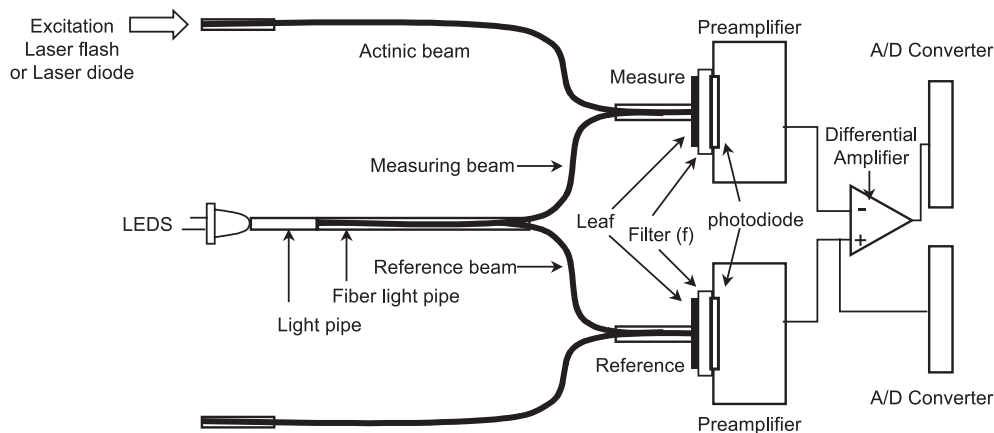


Fig. 1. Spectrophotometric apparatus (see text).

matsu S 3204 (18 × 18 mm). For measurements performed at 485 and 518 nm, the photodiodes are protected from the actinic light by a 6-mm-thick BG 39 Schott filter (f). Owing to the small distance between the leaf and the diode (6 mm), a large fraction of the light scattered by the leaf is collected by the photodiodes. For the measurement performed at 810 nm, the transmitted light is filtered through an 810-nm interference filter (10 nm at half band) and the distance between the photodiodes and the leaf is 60 mm. This optical device decreases the relative intensity of the fluorescence induced by the actinic light with respect to that of the transmitted detecting light.

The LEDs deliver square pulses that are used as detecting flashes; their duration (20 μs) determines the time resolution of the method. Measuring and reference signals are integrated with a time constant of 35 μs and then applied to a differential amplifier (gain = 8). For each detecting flash, the output signal of the differential amplifier is measured by an 18-bit sampling A/D converter (ADC 5020, Analogic Corporation) 3 μs before the flash and at the end of the flash (i.e. 20 μs after the beginning of the flash). The contribution of low frequency noise or parasitic signals is eliminated by computing the difference between the signal measured after and before the flash. A second sampling A/D converter samples at the end of the flash the signal I delivered by the reference photodiode. The changes in the  $\Delta I/I$  ratio are proportional to the absorption changes in the leaf. The signal-to-noise ratio is  $\sim 10^5$ , i.e. slightly improved as compared to that obtained with the xenon flash technique. The major improvement gained with this new technique is the reduction of the time interval between detecting flashes that is now 200 μs, to be compared to 7 ms in the case of the xenon flash technique. This is well demonstrated in the experiments shown in Fig. 3B, in which five detecting flashes are distributed in a time interval of 4 ms. It allows, in a single experiment, an excellent definition of the time course of membrane potential decay. With the xenon flash technique, the same analysis would have required five independent experiments, each of them separated by period of 7-min dark adaptation.

A dye laser pumped by the second harmonic of a Nd Yag laser provides short (8 ns) saturating flashes at 695 nm. Continuous illumination is provided by a 500-mW SDL laser diode with an emission peak at 690 nm. The maximum light intensity provided by the laser diode at the surface of the leaf is  $\sim 1 \times 10^4 \mu\text{E m}^{-2} \text{s}^{-1}$ .

Membrane potential changes were measured as the difference (518–485 nm). This difference eliminates most of the contributions of  $P_{700}$  and *cyt f*, and of the light scattering changes induced by a strong continuous illumination.

Changes in the redox state of  $P_{700}$ , on which is superimposed a contribution of PC, were measured at 810 nm. The time resolution is limited to 300 μs owing to fluorescence signal induced by the actinic illumination.

The leaves were dark-adapted for 7 min and four experiments were averaged at each wavelength.

## 2.2. Computation of the rate of the photochemical reactions

The photochemical rate  $R_{\text{ph}} = R_{\text{PSI}} + R_{\text{PSII}}$ , in which  $R_{\text{PSI}}$  and  $R_{\text{PSII}}$  are the rates of photochemical reactions I and II, respectively, has been determined according to the method described in Ref. [20]. During the illumination period, the rate of membrane potential changes ( $R_{\text{light}}$ ) is proportional to  $R_{\text{ph}} + R_{\text{bf}} - R_{\text{leak}}$ , in which  $R_{\text{bf}}$  is the rate of the membrane potential formation associated with the turnover of the *cyt b/f* complex and  $R_{\text{leak}}$  is the rate of ion leaks (passive or via the ATPsynthase). At the time the light is switched off, the photochemical rates  $R_{\text{PSI}}$  and  $R_{\text{PSII}}$  fall to zero in the sub-microsecond time range. On the contrary, the value of  $R_{\text{bf}}$  that is associated with the reduction of *cyt f* decays slowly in a several-millisecond time range [20]. Thus, the difference between the rate of membrane potential changes measured immediately before and after switching off the light is proportional to  $R_{\text{ph}}$ , according to:

$$R_{\text{light}} - R_{\text{dark}} = R_{\text{ph}} + R_{\text{bf}} - R_{\text{leak}} - (R_{\text{bf}} - R_{\text{leak}}) = R_{\text{ph}}$$

In the experiments depicted in Figs. 2–3 and 5–7, the value of  $R_{\text{light}}$  is negligible compared to  $R_{\text{dark}}$ . Consequently,  $R_{\text{ph}}$  is equal to the rate of the membrane potential decay extrapolated to the time the light is switched off (time zero).

The membrane potential increase measured 100  $\mu\text{s}$  after a short saturating flash is proportional to the concentration of PSI+PSII centers. In the case of spinach leaf, the membrane potential changes induced by a saturating flash are about twice larger in the absence than in the presence of hydroxylamine + DCMU that blocks irreversibly PSII [20], so that the concentration of PSI and PSII centers can be considered as equal. Similar measurements performed by F. Rappaport with Arabidopsis leaves led to similar conclusions (personal communication). Thus, the membrane potential change  $F$  induced by a short saturating flash given to a dark-adapted leaf corresponds to the transfer of two charges per photosynthetic electron chain (one PSI+one PSII charge separation). Membrane potential changes have been divided by  $F/2$ , which corresponds to the transfer of one charge per photosynthetic chain. According to Ref. [28], one charge separation corresponds to a membrane potential increase of  $\sim 25$  mV. This normalization allows expressing  $R_{\text{ph}}$  in terms of the number of charges transferred through the membrane per second and per photosynthetic chain.

The respective photochemical rate constants of PSI and PSII reactions have been estimated by measuring the initial rate of the membrane potential increase induced by a continuous illumination given to dark-adapted material in the absence or in the presence of 2 mM hydroxylamine + 50  $\mu\text{M}$  DCMU. At the highest light energy provided by the laser diode, we estimate the average value of the photochemical rate constant to  $ki_{\text{PSI}} = \sim 9 \times 10^3 \text{ s}^{-1}$  corresponding to one photon trapped per PSI center every 110  $\mu\text{s}$ . At 690 nm (laser diode) and whatever the light

intensity, we have  $ki_{\text{PSII}} = \sim 0.5 ki_{\text{PSI}}$  in agreement with PSI and PSII action spectra.

### 3. Results and discussion

In measurements performed under light intensity higher than  $ki_{\text{PSI}} \sim 6 \times 10^3 \text{ s}^{-1}$  that is saturating for both the linear and cyclic pathways, the electron flux is limited by the rate of dark processes and does not depend on the distribution of light excitation between the two photosystems. During the course of illumination, the concentration of active PSII or PSII centers is close to zero.

Fig. 2 shows the kinetics of the membrane potential decay measured after 150-ms illumination of a dark-adapted leaf at the highest intensity provided by the laser diode (curve 1,  $ki_{\text{PSI}} \sim 9 \times 10^3 \text{ s}^{-1}$ ) and at a lower intensity (curve 2,  $ki_{\text{PSI}} 1.6 \times 10^3 \text{ s}^{-1}$ ). Fluorescence measurement shows that the 150-ms illumination induces a full reduction of the PSII primary acceptor  $Q_A$  and of the PQ pool. The experiment has been performed with the xenon flash technique (time resolution  $\sim 15 \mu\text{s}$ ). Following the illumination, the membrane potential decay displays biphasic kinetics with a fast phase completed in  $\sim 1$  ms. In curve 1, the amplitude of the fast phase corresponds to the transfer across the membrane of 0.28 charge per photosynthetic chain. The overall half time for the fast decaying phase is  $\sim 60 \mu\text{s}$  but the kinetics is better fitted by a two-exponential function ( $t_{1/2} \sim 16$  and  $\sim 190 \mu\text{s}$ ) or by a higher number of exponential functions. In curve 2, the amplitude of the fast phase is  $\sim 5.6$  times smaller than for curve 1, a ratio equal to that of the light intensities.

Fig. 3 shows the membrane potential decay upon a light to dark transfer following a 150-ms illumination of a dark-adapted leaf by the laser diode, with  $ki_{\text{PSI}} = \sim 6 \times 10^3 \text{ s}^{-1}$  (curve 1) or  $ki_{\text{PSI}} = \sim 2.6 \times 10^3 \text{ s}^{-1}$  (curve 2). This experiment was performed using the spectrophotometer in which detecting flashes are provided by LEDs. As already shown in Fig. 2, the extent of the fast phase is proportional to light intensity (Fig. 3B,  $\sim 0.18$  and  $0.09$  for curves 1 and 2, respectively).

Fig. 4 shows absorption changes at 810 nm, measured with the same leaf and under the same experimental conditions as in Fig. 3. During the 150-ms illumination period (Fig. 4A), a fast absorption increase completed in  $\sim 10$  ms is associated with the oxidation of  $P_{700}$  and PC. This oxidation phase is followed by a partial reduction completed in  $\sim 100$  ms previously described in Ref. [29]. Switching off the light leads to further multiphasic reduction of  $P_{700}^+$  and  $PC^+$ , shown on an enlarged scale in Fig. 4B. A fast reduction phase is completed in  $\sim 1$  ms and its amplitude is found proportional to the light intensity as found for the fast phase in the membrane potential decay. The slower phase is roughly independent of light intensity. On these bases, we ascribe the fast phase seen in the 810-nm absorption changes and in the membrane potential decay to a charge

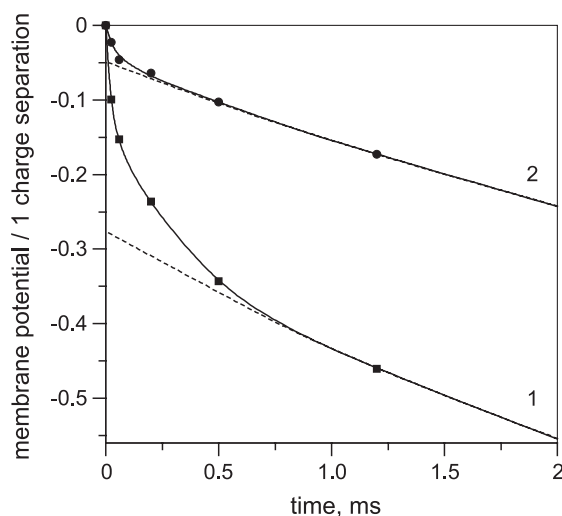


Fig. 2. Membrane potential decay measured after 150-ms illumination of leaves dark-adapted for 7 min. Curve 1,  $ki_{\text{PSI}} = \sim 9 \times 10^3 \text{ s}^{-1}$ . Curve 2,  $ki_{\text{PSI}} = \sim 1.6 \times 10^3 \text{ s}^{-1}$ . The experiment has been performed with the Xenon flash technique over a 9-ms dark period.

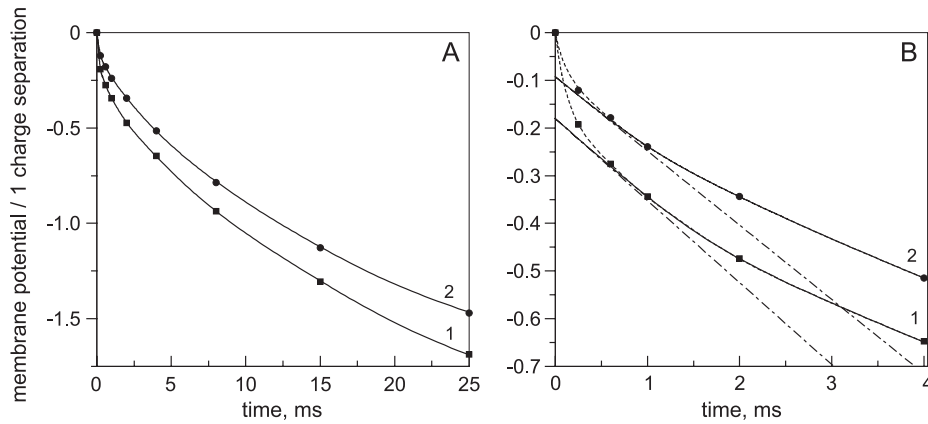
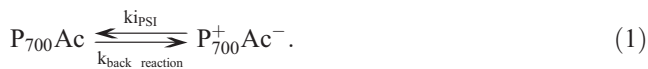


Fig. 3. Membrane potential decay measured after 150-ms illumination of a leaf dark-adapted for 7 min. The experiment has been performed with the LEDS technique. A. Curve 1:  $k_{\text{PSI}} = \sim 6 \times 10^3 \text{ s}^{-1}$ . Curve 2:  $k_{\text{PSI}} = \sim 2.6 \times 10^3 \text{ s}^{-1}$ . B, same results as A, with expanded amplitude and time scales. Dashed lines, fast phase of the membrane potential decay. Solid lines, slow phase of the membrane potential decay extrapolated to time zero. Dash dot lines, initial rate of the slow phase of the membrane potential decay. At the time the light is switched off, the value of the membrane potential normalized to one-charge separation is 3.04 and 3.4 for curves 1 and 2, respectively. These values correspond to absorption changes of  $\Delta I/I \sim 4.1 \times 10^{-3}$  and  $\sim 4.6 \times 10^{-3}$  for curves 1 and 2, respectively.

recombination between  $\text{P}_{700}^+$  and a reduced PSI acceptor  $\text{Ac}^-$  (Eq. (1)):

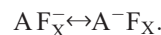


This model predicts that the amplitude of the charge recombination process measured when the light is switched off is proportional to  $k_{\text{PSI}}$ , as shown in Figs. 2–3. In this framework, the extent of the fast membrane potential decay yields the fraction of PSI centers in the  $\text{P}_{700}^+\text{Ac}^-$  state that is  $\sim 0.28$  for the highest light intensity (Fig. 2, curve 1).

### 3.1. Identity of Ac

As discussed in Ref. [30], most of the charge recombination processes that have been characterized in isolated PSI RCs display highly multiphasic kinetics that likely reflect structural heterogeneity of the RCs. Under conditions where the iron sulfur clusters  $\text{F}_X$ ,  $\text{F}_A$  and  $\text{F}_B$  are prereduced, the half time of the charge recombination process involving  $\text{P}_{700}^+$  and

reduced phyloquinone  $\text{A}_1^-$  measured in isolated PSI centers is  $\sim 250 \text{ ns}$  [31]. Charge recombination process with half time of  $\sim 250 \mu\text{s}$  was ascribed to the  $\text{P}_{700}^+\text{F}_X^-$  pair under conditions where  $\text{F}_A$  and  $\text{F}_B$  were prereduced [32]. Much slower charge recombination processes are observed in RCs, in which  $\text{F}_X$  or  $\text{F}_A\text{F}_B$  have been removed by biochemical treatment or by mutagenesis. These conditions, in which no electrostatic interaction occurs between secondary acceptors, are not relevant to in vivo measurements. Half time of 45 ms [33] has been reported for the charge recombination involving  $\text{P}_{700}^+$  and  $\text{F}_A^-$  or  $\text{F}_B^-$ . The comparison between these different rate constants and those we experimentally determined leads us to identify Ac as the iron sulfur cluster  $\text{F}_X$ . Assuming that the charge recombination involving  $\text{F}_X^-$  proceeds via  $\text{A}_1$  [30], the rate of the process will depend upon the equilibrium constant of the reaction



The large membrane potential induced by a continuous illumination will decrease the value of this equilibrium

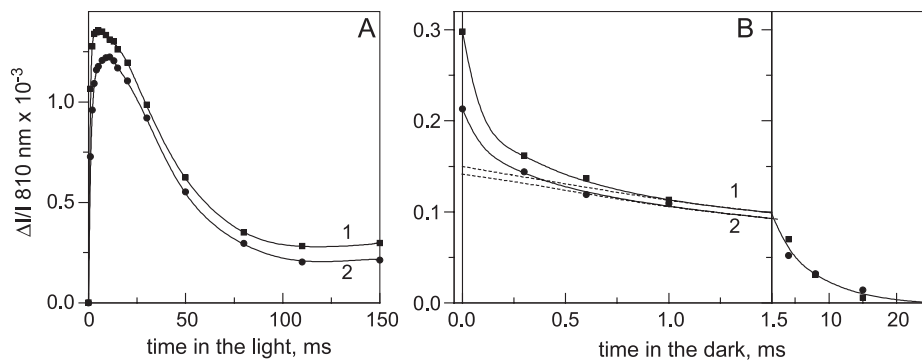


Fig. 4. Kinetics of absorption changes at 810 nm. Same leaf and same experimental conditions as in Fig. 3. (A) Absorption changes measured during the 150-ms illumination. (B) Absorption changes measured in the dark after switching off the light. Dashed lines, extrapolation to time zero of the slow phase of  $\text{P}_{700}^+$  and  $\text{PC}^+$  reduction. Amplitude of the fast phase: 0.148 and 0.072 for curves 1 and 2, respectively.

constant thus increasing both the concentration of  $A_1^-$  and the rate constant of the charge recombination. This could explain why faster charge recombination for the  $P_{700}^+F_X^-$  pair is observed in vivo than in isolated RCs.

Interestingly, the fast phase in the membrane potential decay is not observed under steady-state saturating illumination (not shown). The lack of a charge recombination process suggests that  $F_X$  and likely  $F_A$  and  $F_B$  be in their oxidized form under these conditions. Thus, when the Benson–Calvin cycle is fully activated, the rate of the photosynthetic process would not be limited by the rate of oxidation of PSI acceptors but by the rate of PQH<sub>2</sub> oxidation at site Q<sub>o</sub> of cyt *b/f* complex.

### 3.2. Slow phase in the 810-nm absorption change

The fast phase in the decay of the 810-nm absorption change is followed by a slower phase (Fig. 4B,  $t_{1/2} \sim 4$  ms) roughly independent of the light intensity. This phase is much faster than that expected for a charge recombination process involving  $F_A^-$  or  $F_B^-$  ( $\sim 45$  ms) and is likely associated with the reduction of  $P_{700}^+$  and  $PC^+$  via the cyclic and linear electron transfer chains.

### 3.3. Determination of $R_{ph}$

As discussed in Materials and methods, the photochemical rate  $R_{ph} = R_{PSI} + R_{PSII}$  is equal to the initial rate of the membrane potential decay. As the charge recombination process does not contribute to the net formation of membrane potential, the value of  $R_{ph}$  associated with the linear and cyclic electron flows can only be determined after subtraction of the fast decaying phase of the membrane potential. It is thus proportional to the initial rate of the slow phase that is equal to  $\sim 170$  and  $\sim 159$  s<sup>-1</sup> for curves 1 and 2, respectively (Fig. 3B, dash dot lines). Thus,  $R_{ph}$  decreases by  $\sim 7\%$  when the light intensity is decreased by a factor  $\sim 2.3$ . Similar dependence of the decay rate upon the light intensity is observed during the first 25 ms of dark (Fig. 3A). We thus conclude that the light intensity  $ki_{PSI} = \sim 6 \times 10^3$  s<sup>-1</sup> is saturating for both the cyclic and linear processes. Under saturating excitation for linear and cyclic flows, the concentration of RCs in the photochemically inactive state  $P_{700}^+Ac^-$  increases as a function of the light intensity (Eq. (1)).

The values computed here for  $R_{ph}$  are significantly higher than that reported in [20], i.e.  $\sim 117$  s<sup>-1</sup>. This difference can be ascribed to the higher light intensity and to the better homogeneity of actinic illumination because of the lower chlorophyll content of Arabidopsis leaf compared to spinach. Moreover, the kinetics of the membrane potential decay is defined with a better accuracy owing to the larger number of detecting flashes used with the LEDs technique than in the experiments reported in Ref. [20].

Similar experiments as that described in Fig. 3 have been performed with longer times of illumination.  $R_{ph}$  increases

by  $\sim 10\%$  during the first seconds of illumination and stays constant between 1-s and 8-s illumination (not shown).

### 3.4. Rate of the cyclic flow

The photochemical rate  $R_{ph}$  determined by the initial rate of the slow phase is the sum of the rate of the linear and cyclic flows according to the equation  $R_{ph} = R_{PSII} + R_{PSI \text{ linear}} + R_{cyclic}$ . By definition,  $R_{PSI \text{ linear}} = R_{PSII}$  so that  $R_{ph} = 2R_{PSII} + R_{cyclic}$ . Thus,

$$R_{cyclic} = R_{ph} - 2R_{PSII}. \quad (2)$$

The rate  $R_{PSII}$  (or  $R_{PSI \text{ linear}}$ ) is limited by the rate of the Benson–Calvin cycle mainly deactivated in dark-adapted leaves, and by the rate of the Melher reaction. Electron flux through PSII has been estimated from measurement of the fluorescence yield, which is linearly related to the rate of PSII photoreaction. With spinach leaves [20] under subsaturating illumination,  $R_{PSII} = \sim 13$  s<sup>-1</sup>. As  $R_{PSII}$  is limited by a slow dark process, its value is expected to be similar under subsaturating or saturating light. The same type of measurement performed with Arabidopsis has led to a value of  $R_{PSII} \sim 20$  s<sup>-1</sup> that stays constant between 2 and 4 s of illumination (not shown). Such a rate corresponds to  $\sim 1/10$ th of the maximum rate of linear electron flow when measured under conditions where the Benson–Calvin cycle is fully activated ( $\sim 200$  s<sup>-1</sup>) (G. Johnson, personal communication).

From Eq. (2), we have  $R_{cyclic} = \sim 170$  s<sup>-1</sup>  $- 2 \times \sim 20$  s<sup>-1</sup>  $= \sim 130$  s<sup>-1</sup> for  $ki_{PSI} = 6 \times 10^3$  s<sup>-1</sup> (Fig. 3B, curve 1) and  $R_{cyclic} = \sim 159$  s<sup>-1</sup>  $- 2 \times 20$  s<sup>-1</sup>  $= \sim 119$  s<sup>-1</sup> for  $ki_{PSI} = 2.6 \times 10^3$  s<sup>-1</sup> (Fig. 3B, curve 2).

Under saturating light excitation, most of the excitation collected by PSI antenna is lost, being trapped by inactive RCs such as those in  $P_{700}^+$  or in  $P_{700}F_XF_A^-F_B^-$  states that undergo a rapid charge recombination after capture of an exciton.

### 3.5. Effect of DCMU

We previously reported [20] that an efficient cyclic process is transiently observed in the presence of DCMU, i.e. in conditions where no contribution of the linear pathway occurs. In a further characterization of this effect, we have observed that the rate of the cyclic pathway is highly dependent on the degree of hydration of the leaf, both in the case of spinach and Arabidopsis.

In Fig. 5, the plants were heavily watered for 2 days prior to the experiment. Leaves were infiltrated with either 0.15 M sorbitol + 40  $\mu$ M DCMU (curve 1) or water + 40  $\mu$ M DCMU (curve 2). Fig. 5A shows the membrane potential changes induced by a period of 7-s saturating illumination given to a dark-adapted leaf. In the presence of sorbitol + DCMU, one observes a fast increase of the membrane potential completed in  $\sim 20$  ms (Fig. 5B, enlarged time

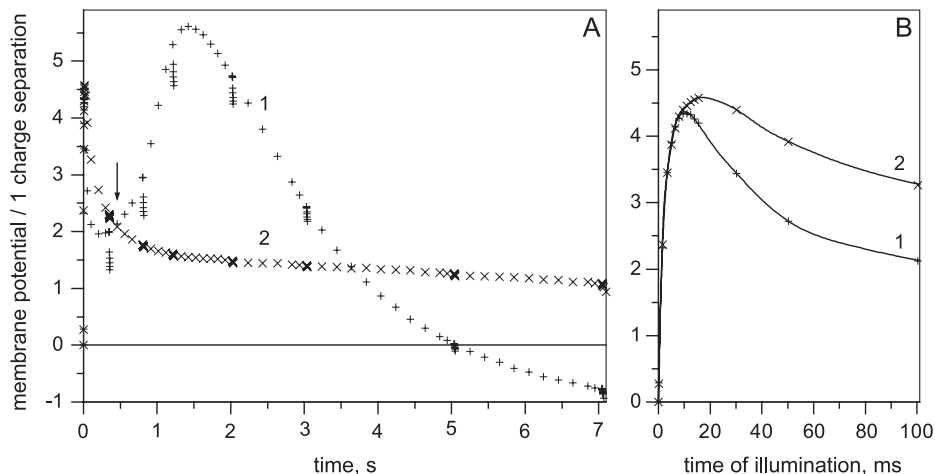


Fig. 5. (A) Kinetics of membrane potential changes induced by 7-s illumination ( $k_{\text{PSII}} = \sim 6 \times 10^3 \text{ s}^{-1}$ ) in the presence of 40  $\mu\text{M}$  DCMU. The light is switched off for 9 ms at times 0.35, 0.8, 1.2, 2, 3, 5 and 7 s. Curve 1: the leaf is infiltrated with 0.15 M sorbitol + 40  $\mu\text{M}$  DCMU. Curve 2: the leaf is infiltrated with water + 40  $\mu\text{M}$  DCMU. The arrow indicates a crossing point of curves 1 and 2. (B) Same data as A, with enlarged time scale.

scale). The extent of this initial increase corresponds to the transfer of at least  $\sim 5$  charges per photosynthetic chain across the membrane. This number is close to the number of primary and secondary PSI donors ( $P_{700}$ , PC, cyt *f* and Rieske protein) that have been reduced during the dark adaptation of the leaf. Their oxidation is completed in  $\sim 20$  ms, owing to the fast electron transfer reaction between these different donors. After a transitory decay, one observes a large increase of the membrane potential that peaks at  $\sim 1.5$  s of illumination (Fig. 5A). This increase must be associated with the occurrence of an efficient PSI-sensitized electron flow related to a cyclic process. This second peak of membrane potential is followed by a slow decay that reveals a progressive inactivation of the cyclic pathway. Assuming that one-charge separation induces a membrane potential increase of  $\sim 25$  mV [28], the peak value of the membrane potential is  $\sim 140$  mV above the dark-adapted level.

When a leaf of the same plant is infiltrated with water + DCMU (Fig. 5B, curve 2) the extent and the kinetics of the first membrane potential increase is similar to that observed in the presence of sorbitol + DCMU. This implies that PSI donors are in similar redox states in the presence or in the absence of sorbitol. On the other hand, the second peak of membrane potential is absent, thus showing that the cyclic flow is not operating in water-infiltrated leaf (Fig. 5A, curve 2).

In order to sample  $R_{\text{ph}}$  during the course of the 7-s illumination, the light was switched off for seven periods of 9 ms (see legend of Fig. 5A). In Fig. 6, the initial rate of the slow phase in the membrane potential decay has been computed for each of the 9-ms dark periods given during the course of illumination, according to the method described in Fig. 3B.  $R_{\text{ph}}$  reaches a maximum value after  $\sim 1$ -s illumination, a time shorter than that of the second membrane potential peak ( $\sim 1.5$ -s illumination).  $R_{\text{ph}}$  can be

ascribed to the cyclic electron flow since  $R_{\text{PSII}}$  is cancelled by the addition of DCMU. The peak value ( $\sim 128 \text{ s}^{-1}$ ) is close to  $R_{\text{cyclic}}$  determined in the absence of DCMU ( $\sim 130 \text{ s}^{-1}$ ).  $R_{\text{ph}}$  decreases to a value close to zero in a time range of a few seconds. As proposed in Ref. [20], we ascribe this decrease to a full oxidation of all the carriers involved in the cyclic pathway through a slow electron leak toward the Benson–Calvin cycle and  $\text{O}_2$  via the Melher reaction. The bound area below curve 1 yields the number of electrons transferred via the cyclic pathway during the 7-s illumination. This value ( $\sim 330$  electrons) is  $\sim 50$  times larger than the size of the pool of reduced PSI donors present at the onset of illumination, which implies that this high photochemical activity cannot be ascribed to the reoxidation of this pool.

In the case of a leaf infiltrated with water + DCMU (Fig. 6, curve 2),  $R_{\text{ph}}$  stays at a low value ( $\sim 5 \text{ s}^{-1}$ ) during the

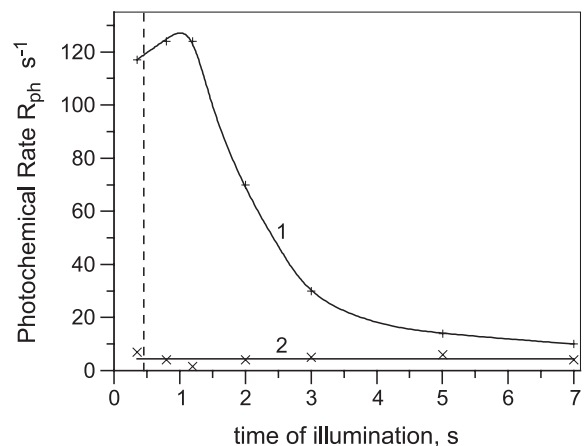


Fig. 6. Photochemical rate  $R_{\text{ph}}$ , computed from Fig. 5A for each of the 9-ms dark periods as a function of the time of illumination. The initial rate of the slow membrane potential decay has been computed as shown in Fig. 3B. Dashed line: crossing point of curves 1 and 2, Fig. 5A.

course of illumination, thus showing that the cyclic flow is operating at a very slow rate. After  $\sim 0.45$ -s illumination, the values of the membrane potential are equal with or without sorbitol (Fig. 5A, arrow) whereas the initial rate of the membrane potential decay is  $\sim 25$  times larger (Fig. 6, dashed line) in the presence than in the absence of sorbitol. The fast membrane potential decay measured in the presence of sorbitol+DCMU reflects a rapid proton leak through the membrane, which implies that a proton gradient was generated during the 0.45-s illumination. This proton gradient activates the ATPase and increases the driving force that induces the proton leak. It is worth noting that, in the presence of sorbitol+DCMU and beyond 5-s illumination, the membrane potential reaches a negative value (Fig. 5A, curve 1). As shown in Ref. [34], such an electric field inversion is associated with the dissipation of the proton gradient, which in the presence of sorbitol + DCMU has been generated by the cyclic flow during the first seconds of illumination.

We propose that the inhibition of the cyclic flow observed in the presence of water+DCMU is associated with an osmotic shock that induces a swelling of the chloroplast and of the lumenal compartment. This osmotic shock is prevented by the addition of 0.15 M sorbitol, a concentration close to being isotonic with the cell. Surprisingly, when the plant is submitted to a moderate drought stress, an efficient cyclic electron flow is observed even when the plant is infiltrated with water+DCMU. This was very likely the case in the experiment reported Fig. 2 in Ref. [20]. Consistent with this, Golding, Finazzi and Johnson (personal communication) have noted the formation of a stable “cyclic-activated” state in barley leaves exposed to drought.

Fig. 7 shows the kinetics of the membrane potential decay after 325-ms and 2-s illumination (curves 1 and 2, respectively) of a leaf infiltrated with 0.15 M sorbitol+40  $\mu$ M DCMU. The kinetics of membrane potential decay displays a fast phase, similar to that observed in the control (Fig. 3B). For curve 1, the amplitude of this phase ( $\sim 0.1$ ) is about the half of that measured in the control ( $\sim 0.18$ , Fig. 3B, curve 1). In the presence of DCMU, which blocks the electron flow from PSII, the  $F_A$  and  $F_B$  acceptors associated with PSI contributing to the linear flow should be oxidized by electron transfer to the Benson–Calvin cycle. These centers cannot contribute to the charge recombination process, which explains the decrease of the amplitude of the fast phase. Increasing the time of illumination decreases the amplitude of both the fast and slow phases of the membrane potential decay (Fig. 7, curves 1 and 2).

### 3.6. Mechanism of cyclic electron transfer

A major conclusion drawn from our experiments is the high rate of the cyclic electron flow that is measured during the first seconds of illumination of dark-adapted

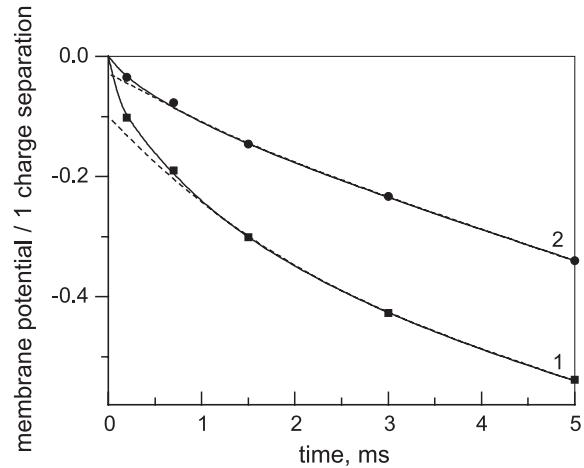


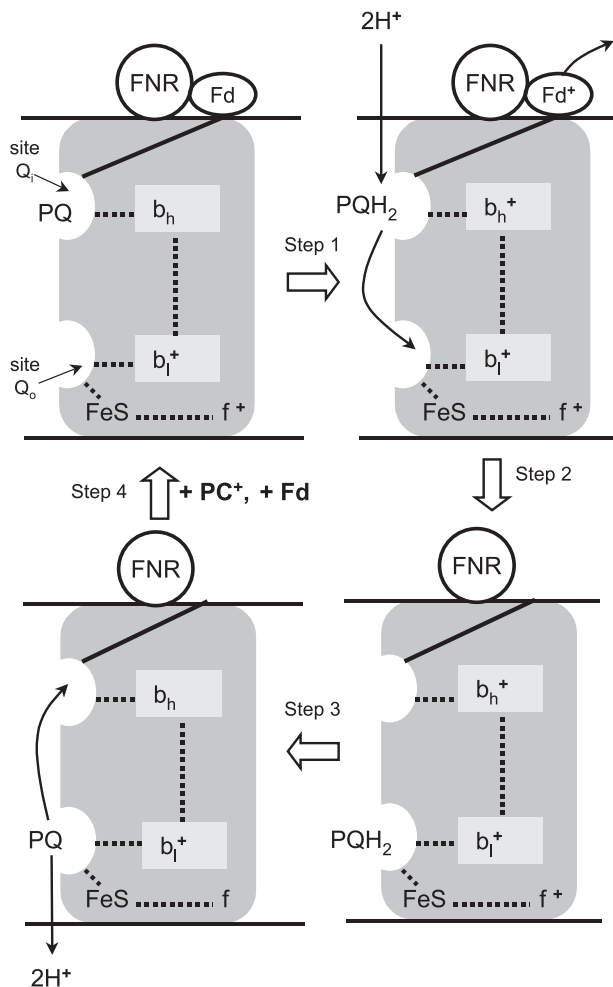
Fig. 7. Kinetics of the membrane potential decay measured after 350-ms (curve 1) and 2-s (curve 2) illumination ( $k_{\text{PSI}} = \sim 6 \times 10^3 \text{ s}^{-1}$ ). The experiment is performed with a different leaf than that in Fig. 5. Dashed lines: extrapolation to time zero of the slow phase of the membrane potential decay. Amplitude of the fast phase:  $\sim 0.1$  and  $\sim 0.03$  for curves 1 and 2, respectively.

leaves. There is a general agreement that PSI and *cyt b/f* complexes are involved in the cyclic process but the mechanism of electron transfer from the acceptor side of PSI to the *cyt b/f* complex has not yet been clearly identified. According to a conventional Q-cycle process [35,36], electrons can be transferred to the *cyt b/f* only via a plastoquinol ( $\text{PQH}_2$ ), bound at site  $Q_0$ . In this case, the cyclic process obligatorily involves an enzyme able to transfer electron from the acceptor side of PSI to PQ. A gene coding for such an enzyme (NADP-dehydrogenase, NDH), similar to the mitochondrial complex I, has been identified in the genome of higher plants [37] but biochemical analyses have shown that the concentration of this enzyme is much lower ( $\sim 1\%$ ) than that of the photosynthetic electron transfer chain [38]. If the concentration of NDH is a few percent of that of PSI, this enzyme should operate at a rate of  $\sim 10^4 \text{ s}^{-1}$  to sustain a rate of cyclic electron flow of  $130 \text{ s}^{-1}$ . It is unlikely that NDH could operate at such high rate but it does not exclude that it could contribute to slow processes of cyclic electron flow, for instance under weak far red excitation [14]. In the case of the cyclic flow measured under strong illumination, we thus favor the hypothesis that, unlike in a conventional Q-cycle process, electrons are directly transferred from the acceptor side of PSI to *cyt b/f* complex via a site localized on its stromal side, as already proposed in Refs. [21,39]. It is very likely that the same mechanism is involved in the process of electron transfer between PSI acceptors and *cyt b/f* in the cyclic phosphorylation process characterized by Arnon and coworkers in isolated thylakoid membranes. Interestingly, an efficient cyclic phosphorylation can be induced by the addition of various soluble electron carriers as vitamin K, flavine mononucleotide or PMS instead of Fd, as reviewed in Ref. [40]. This suggests that, in vitro,

the process of electron transfer from the acceptor side of PSI to cyt *b/f* complex does not involve a specific binding site, as it would likely be the case for NDH.

It has been shown that Fd-NADP reductase (FNR) copurifies with the cyt *b/f* complex [41,42]. We thus propose that the FNR–cyt *b/f* complex is able to bind the reduced Fd, formed at the level of PSI center. This reduced Fd would transfer electron to a PQ bound at site  $Q_i$ . We propose (Scheme 1) a tentative mechanism in which the cyt *b/f* catalyzes the electron transfer from Fd to PC by a process that leads to the pumping of one proton per electron transferred.

In this model, both  $Q_o^-$  and  $Q_i^-$  sites behave in a quite symmetric way. At site  $Q_o$ , two electrons are transferred from  $PQH_2$ , one to the *b*-cyts chain and the other to the soluble PC via the high potential chain (FeS cyt *f*). At site  $Q_i$ , two electrons are transferred to a bound PQ. One electron is transferred from Fd via an electron transfer chain



Scheme 1. Mechanism for electron transfer within the cyt *b/f* complex. Dotted lines, electron pathway in a conventional Q-cycle process, involved in both linear and cyclic pathways. Solid line, electron transfer pathway that connects the stromal side of cyt *b/f* complex to site  $Q_i$  involved in cyclic pathway only.  $b_h$ ,  $b_l$ , high potential and low potential *b*-cyts in the cyt *b/f* complex.

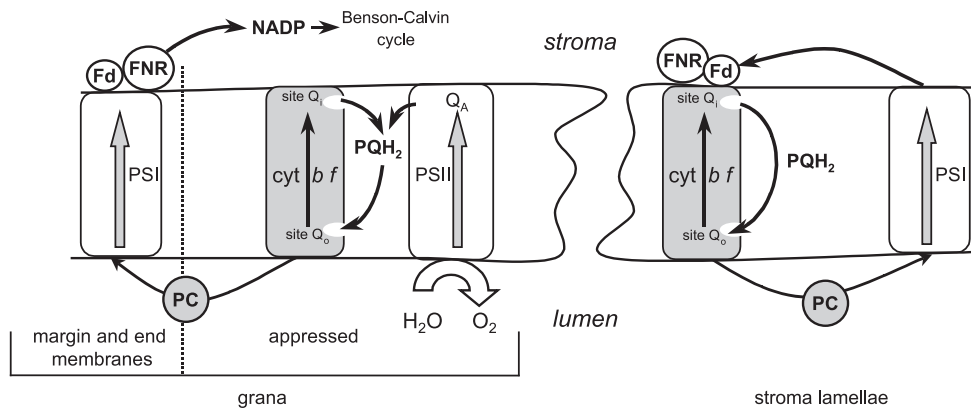
not yet characterized and a second electron is transferred from cyt  $b_h$  to PQ. The occurrence of such a “reductant-induced” oxidation of cyt *b* has been previously proposed [43]. In this mechanism, PQ acts as a catalyst that is permanently recycled between the  $Q_i$  and the  $Q_o$  sites. Interestingly, this process leads to the transfer of one charge across the membrane per  $PC^+$  as in a classical Q-cycle process. The main difference between cyt *b/f* and cyt *b/c* complex would be that cyt *b/c* operates exclusively according to the classical Q-cycle process while cyt *b/f* possesses an additional electron pathway, which connects its stromal side to site  $Q_i$ .

A new covalently bound cytochrome *c'* has been recently identified in the structure of the cyt *b/f* complex [44,45]. This cytochrome, localized on the stromal side of cyt  $b_h$  and in its immediate vicinity, could be very likely involved in the electron chain that establishes a link between the stromal side of the cyt *b/f* complex and site  $Q_i$ .

### 3.7. Spatial organization of the electron transfer chain within the thylakoid membrane

Grant and Whatley [46] and Allen [47] pointed out that the efficiency of the cyclic pathway around PSI is controlled by the redox poise of the carriers involved in this process, and more specifically, by the redox state of the donors or acceptors of PSI. The redox poise is determined by the relative input and output rates of electron transfer between the carriers involved in the cyclic flow and the soluble carriers localized either in the stromal or the luminal compartments. Consequently, the large efficiency of the cyclic pathway observed during the first seconds of illumination obligatorily requires that the carriers involved in the cyclic and linear chains be structurally separated in order to limit the rate of electron exchange between these two pathways. If cyclic and linear pathways were able to rapidly exchange electrons, the high reductive power generated by PSII activity and the slow rate of electron output via the Benson–Calvin cycle would lead to an overreduction of all carriers. On the other hand, in the presence of DCMU, the Benson–Calvin cycle, although operating at a slow rate, will induce in a few hundreds of ms a full oxidation of all carriers involved in cyclic and linear pathways. Reduction of PSI acceptors in the absence of DCMU, or oxidation of  $P_{700}$  in its presence, both will lead to the inactivation of all PSI centers.

In a first class of hypotheses [20–23], the carriers involved in the cyclic pathway are associated to form a supercomplex including PSI centers, cyt *b/f* complex, FNR, a bound PC and a bound Fd. The swelling of the luminal compartment induced by infiltration of water would lead to a decrease of PC concentration in the lumen and therefore, to a release of the PC bound to the supercomplexes in the luminal compartment. Under this condition, cyclic and linear chains are no more isolated one from the other. In the presence of DCMU, reduced PC localized in the lumen



Scheme 2. Localization of the cyclic and linear electron transfer chains, based on the model proposed in Ref. [50].

will be able to transfer electron to all PSI centers, including the “linear PSI”. This would lead to a rapid oxidation of all carriers and, consequently, to the inhibition of the cyclic process.

A second class of hypotheses does not imply a permanent association between the membrane proteins involved in the cyclic flow. A structural model of the organization of the thylakoid membrane has been proposed on the basis of a detailed biochemical analysis of different membrane fragments [48–50]. In these models, the PSI centers that participate to the linear and cyclic electron flows are localized in different membrane regions (Scheme 2). A large fraction of the PSI centers is included in the margin [51] and in the ends of the grana stacks. These PSI centers, localized at short distance of the appressed region, would be preferentially involved in the linear pathway. The other fraction of the PSI centers, localized in the stroma lamellae, would be preferentially involved in the cyclic pathway. FNR could play a key role in the discrimination between PSI centers involved in cyclic and linear flow (“PSI cyclic” and “PSI linear”, respectively). It has been shown that a small hydrophilic polypeptide is involved in the binding of FNR and Fd to PSI [52]. As the formation of such a complex increases the efficiency of NADP reduction [53], we suggest that FNR-bound “linear PSI” favor rapid electron transfer toward the Benson–Calvin cycle. On the other hand, in membrane region where cyclic flow is operating, FNR would preferentially bind the cyt *b/f* complex and not the “cyclic PSI” that will prevent rapid electron leaks toward the Benson–Calvin cycle. In this model, the pool of soluble Fd, photoreduced by “cyclic PSI”, is reoxidized at the level of the cyt *b/f* localized in the non-appressed regions (Scheme 1). Water infiltration would induce the swelling of the chloroplast compartment and a decrease of the Fd concentration that leads to the inhibition of cyclic electron flow.

A detailed analysis of the kinetics and stoichiometry of electron transfer between  $P_{700}$  and cyt *f* under flash excitation should provide key information on the structural organization of the primary and secondary PSI donors and

could permit to operate a choice between models involving supercomplexes or freely diffusing soluble carriers.

## Acknowledgements

This work was supported by the Centre National de la Recherche Scientifique (Unité Propre de Recherche 1261) and the Collège de France. The authors are indebted to G. Johnson and F. Rappaport for their critical reading of the manuscript.

## References

- [1] D.I. Arnon, F.R. Whatley, M.B. Allen, Vitamin K as a cofactor of photosynthetic phosphorylation, *Biochim. Biophys. Acta* 16 (1955) 607–608.
- [2] A.T. Jagendorf, M. Avron, Cofactors and rates of photosynthetic phosphorylation by spinach chloroplasts, *J. Biol. Chem.* 231 (1958) 277–290.
- [3] K. Tagawa, H.Y. Tsujimoto, D.I. Arnon, Role of chloroplast ferredoxin in the energy conversion process of photosynthesis, *Proc. Natl. Acad. Sci. U. S. A.* 49 (1963) 567–572.
- [4] K. Tagawa, D.I. Arnon, Ferredoxins as electron carriers in photosynthesis and in the biological production and consumption of hydrogen gas, *Nature* 195 (1962) 537–543.
- [5] D.S. Bendall, R.S. Manasse, Cyclic photophosphorylation and electron transport, *Biochim. Biophys. Acta* 1229 (1995) 23–38.
- [6] J.F. Allen, Cyclic, pseudocyclic and noncyclic photophosphorylation: new links in the chain, *Trends Plant Sci.* 8 (2003) 15–19.
- [7] A.T. Mehler, Studies on reactions of illuminated chloroplasts: I. Mechanism of the reduction of oxygen and other Hill reagents, *Arch. Biochem. Biophys.* 33 (1951) 65–77.
- [8] M.R. Badger, Photosynthetic oxygen exchange, *Annu. Rev. Plant Physiol.* 36 (1985) 27–53.
- [9] J. Harbinson, C.H. Foyer, Relationships between the efficiencies of Photosystem-I and Photosystem-II and stromal redox state in  $CO_2$ -free air—Evidence for cyclic electron flow in vivo, *Plant Physiol.* 97 (1991) 41–49.
- [10] U. Gerst, U. Schreiber, S. Neimanis, U. Heber, Photosynthesis: from light to biosphere, in: P. Mathis (Ed.), *Proc. Xth International Photosynthesis Congress*, vol. II, Kluwer Academic Publishing, Montpellier, 1995, pp. 835–838.

- [11] C. Klughammer, U. Schreiber, An improved method, using saturating light-pulses, for the determination of Photosystem-I quantum yield via  $P_{700}^+$  absorbency changes at 830 nm, *Planta* 192 (1994) 261–268.
- [12] J.E. Clarke, G.N. Johnson, In vivo temperature dependence of cyclic and pseudocyclic electron transport in barley, *Planta* 212 (2001) 808–816.
- [13] G. Comic, J.M. Briantais, Partitioning of photosynthetic electron flow between  $\text{CO}_2$  and  $\text{O}_2$  reduction in a  $\text{C}_3$  leaf (*Phaseolus vulgaris* L.) at different  $\text{CO}_2$  concentrations and during drought stress, *Planta* 183 (1991) 178–184.
- [14] T. Joët, L. Courmac, G. Peltier, M. Havaux, Cyclic electron flow around photosystem I in C-3 plants. In vivo control by the redox state of chloroplasts and involvement of the NADH–dehydrogenase complex, *Plant Physiol.* 128 (2002) 760–769.
- [15] B. Andersson, J.M. Anderson, Lateral heterogeneity in the distribution of chlorophyll–protein complexes of the thylakoid membranes of spinach chloroplasts, *Biochim. Biophys. Acta* 593 (1980) 427–440.
- [16] R.P. Cox, B. Andersson, Lateral and transverse organisation of cytochromes in the chloroplast thylakoid membrane, *Biochem. Biophys. Res. Commun.* 103 (1981) 1336–1342.
- [17] P. Joliot, J. Lavergne, D. Béal, Plastoquinone compartmentation in chloroplasts: 1. Evidence for domains with different rates of photo-reduction, *Biochim. Biophys. Acta* 1101 (1992) 1–12.
- [18] J. Lavergne, J.P. Bouchaud, P. Joliot, Plastoquinone compartmentation in chloroplasts: 2. Theoretical aspects, *Biochim. Biophys. Acta* 1101 (1992) 13–22.
- [19] H. Kirchhoff, S. Horstmann, E. Weis, Control of the photosynthetic electron transport by PQ diffusion microdomains in thylakoids of higher plants, *Biochim. Biophys. Acta* 1459 (2000) 148–168.
- [20] P. Joliot, A. Joliot, Cyclic electron transfer in plant leaf, *Proc. Natl. Acad. Sci. U. S. A.* 99 (2002) 10209–10214.
- [21] N. Carillo, R.H. Vallejos, The light-dependent modulation of photosynthetic electron transport, *TIBS* 1983 (1983 February) 52–56.
- [22] A. Laisk, V. Oja, U. Heber, Steady-state and induction kinetics of the photosynthetic electron transport related to donor side oxidation and acceptor side reduction of photosystem I in sunflower leaves, *Photosynthetica* 27 (1992) 449–463.
- [23] A. Laisk, Mathematical modelling of free-pool and channelled electron transport in photosynthesis: evidence for a functional super-complex around photosystem I, *Proc. R. Soc. Lond., B* 251 (1993) 243–251.
- [24] U. Heber, D. Walker, Concerning a dual function of coupled cyclic electron-transport in leaves, *Plant Physiol.* 100 (1992) 1621–1626.
- [25] A. Sacksteder, D.M. Kramer, Dark-interval relaxation kinetics (DIRK) of absorbance changes as a quantitative probe of steady-state electron transfer, *Photosynth. Res.* 66 (2000) 145–158.
- [26] P. Joliot, D. Béal, B. Frilley, Une nouvelle méthode spectrophotométrique destinée à l'étude des réactions photosynthétiques, *J. Chim. Phys.* 77 (1980) 209–216.
- [27] P. Joliot, A. Joliot, Electron transfer between the two photosystems: I. Flash excitation under oxidizing conditions, *Biochim. Biophys. Acta* 765 (1984) 210–218.
- [28] H.T. Witt, Energy conversion in the functional membrane of photosynthesis. Analysis by light pulse and electric pulse methods. The central role of the electric field, *Biochim. Biophys. Acta* 505 (1979) 355–427.
- [29] R.J. Strasser, G. Schansker, A. Srivastava, Govindjee, in: C. Critchley (Ed.), PS2001 12th International Congress on Photosynthesis, CSIRO Publishers, Brisbane, Australia, 2001, pp. S14–S103.
- [30] V.P. Shinkarev, B. Zybailov, I.R. Vassiliev, J.H. Golbeck, Modeling of the  $P_{700}^+$  charge recombination kinetics with phyloquinone and plastoquinone-9 in the A1 site of photosystem I, *Biophys. J.* 83 (2002) 2885–2897.
- [31] P. Sétif, K. Brettel, Photosystem I photochemistry under highly reducing conditions: study of the  $P_{700}$  triplet state formation from the secondary radical pair ( $P_{700}^{\cdot-}$ - $A_1^{\cdot}$ ), *Biochim. Biophys. Acta* 1020 (1990) 232–238.
- [32] P. Sétif, K. Brettel, Forward electron transfer from phyloquinone  $A_1$  to iron–sulfur centers in spinach Photosystem I, *Biochemistry* 32 (1993) 7846–7854.
- [33] T. Hiyama, B. Ke, A further study of P430. A possible primary acceptor of photosystem I, *Arch. Biochem. Biophys.* 147 (1971) 99–180.
- [34] J.A. Cruz, C.A. Sacksteder, A. Kanazawa, D.M. Kramer, Contribution of electric field ( $\Delta\psi$ ) to steady-state transthylakoid proton motive force ( $pmf$ ) in vitro and in vivo. Control of  $pmf$  parsing into ( $\Delta\psi$ ) and ( $\Delta\psi$ )pH by ionic strength, *Biochemistry* 40 (2001) 1226–1237.
- [35] P. Mitchell, The protonmotive Q cycle: a general formulation, *FEBS Lett.* 59 (1975) 137–199.
- [36] A.R. Crofts, S.W. Meinhardt, K.R. Jones, M. Snozzi, The role of the quinone pool in the cyclic electron-transfer chain of *Rhodospseudomonas spaeroides*. A modified Q-cycle mechanism, *Biochim. Biophys. Acta* 723 (1983) 202–218.
- [37] K. Shinokazi, M. Ohme, M. Tanaka, T. Wakasaki, N. Hayashida, T. Matsubayashi, N. Zaita, J. Chunwongse, J. Obokata, K. Yamaguchi-Shinokazi, C. Ohto, K. Torazawa, B.Y. Meng, M. Sugita, H. Deno, T. Kamogashira, K. Yamada, J. Kusuda, F. Takaiwa, A. Kato, N. Tohdoh, H. Shimada, M. Sugiura, The complete nucleotide sequence of the tobacco chloroplast genome: its gene organization and expression, *EMBO J.* 5 (1986) 2043–2049.
- [38] L.A. Sazanov, P. Burrows, P.J. Nixon, Photosynthesis: from light to biosphere, in: P. Mathis (Ed.), Xth Int. Cong. on Photosynthesis, vol. 2, Kluwer Academic Publishing, Montpellier, France, 1995, pp. 705–708.
- [39] W.A. Cramer, P.N. Furbacher, A. Szczepaniak, G.S. Tae, Current Topics in Bioenergetics, vol. 16, Academic Press Inc., 1991, pp. 179–222.
- [40] D.I. Arnon, in: W.D. Mc Elroy, B. Glass (Eds.), *Light and Life*, The John Hopkins Press, Baltimore, 1961, pp. 489–569.
- [41] R.D. Clark, M.J. Hawkesford, S.J. Coughlan, J. Bennett, G. Hind, Association of ferredoxin NADP+ oxidoreductase with the chloroplast cytochrome  $b-f$  complex, *FEBS Lett.* 174 (1984) 137–142.
- [42] H.M. Zhang, J.P. Whitelegge, W.A. Cramer, Ferredoxin: NADP(+) oxidoreductase is a subunit of the chloroplast cytochrome  $b(6)f$  complex, *J. Biol. Chem.* 276 (2001) 38159–38165.
- [43] R.K. Chain, Evidence for a reductant-dependent oxidation of chloroplast cytochrome  $b-563$ , *FEBS Lett.* 143 (1982) 273–278.
- [44] G. Kurisu, H.M. Zhang, J.L. Smith, W.A. Cramer, Structure of the cytochrome  $b_6f$  complex of oxygenic photosynthesis: tuning the cavity, *Science* 302 (2003) 1009–1014.
- [45] D. Stroebel, Y. Choquet, J.-L. Popot, D. Picot, An atypical haem in the cytochrome  $b_6f$  complex, *Nature* 426 (2003) 413–418.
- [46] B.R. Grant, F.R. Whatley, in: T.W. Goodwin (Ed.), *Biochemistry of Chloroplasts*, vol. 2, Academic Press, New York, 1967, pp. 505–511.
- [47] J.F. Allen, Regulation of photosynthetic phosphorylation, *CRC Crit. Rev. Plant Sci.* 1 (1983) 1–22.
- [48] J.M. Anderson, The grana margins of plant thylakoid membranes, *Physiol. Plant.* 76 (1989) 243–248.
- [49] P.A. Albertsson, The structure and function of the chloroplast photosynthetic membrane—A model for the domain organization, *Photosynth. Res.* 46 (1995) 141–149.
- [50] P.A. Albertsson, A quantitative model of the domain structure of the photosynthetic membrane, *Trends Plant Sci.* 6 (2001) 349–354.
- [51] A.N. Webber, K.A. Platt-Aloia, R.L. Heath, W.W. Thomson, The marginal regions of thylakoid membranes: a partial characterization by polyoxyethylene sorbitane monolaurate (Tween 20) solubilization of spinach thylakoids, *Physiol. Plant.* 72 (1988) 288–297.
- [52] H. Scheller, P. Jensen, A. Haldrup, C. Lunde, J. Knoetzel, Role of subunits in eukaryotic Photosystem I, *Biochim. Biophys. Acta* 1507 (2001) 41–60.
- [53] H. Naver, N. Scott, B. Andersen, B. Moller, H. Scheller, Reconstitution of barley photosystem-I reveals that the N-terminus of the PSI-D subunit is essential for tight-binding of PSI-C, *Physiol. Plant.* 95 (1995) 19–26.